Structure of the chiral smectic-C^*_α phase

D. Schlauf and Ch. Bahr*
Institute of Physical Chemistry, University Marburg, D-35032 Marburg, Germany

H. T. Nguyen
Centre de Recherche Paul Pascal, Avenue A. Schweitzer, F-33600 Pessac, France

(Received 3 June 1999)

Ellipsometric measurements of freely suspended films of a chiral liquid-crystal compound possessing the phase sequence smectic-A–smectic-C^*_α–smectic-C^* have been conducted in order to elucidate the structure of the smectic-C^*_α phase. The measured ellipsometric quantities Δ and Ψ are compared with values, which were calculated for model films using the 4×4 matrix method. Our results confirm, for the compound under investigation, predictions of a phenomenological model [M. Čepič and B. Žekš, Mol. Cryst. Liq. Cryst. **263**, 61 (1995)] according to which the smectic-C^*_α phase is characterized by a short-pitch helical structure. [S1063-651X(99)16711-4]

PACS number(s): 61.30.Gd, 64.70.Md

I. INTRODUCTION

Smectic-C (Sm-C) liquid-crystal phases can be considered as stacks of molecular layers, each layer corresponding to a two-dimensional liquid in which the rodlike molecules tend to align along a common direction, denoted by the director $\vec{n}$, which is inclined by a tilt angle of (temperature dependent) magnitude θ with respect to the layer normal $\vec{z}$. If the constituent molecules are chiral, a spontaneous electric polarization $\vec{P}_s$ is present in each layer of the chiral Sm-C^* phase. The direction of $\vec{P}_s$ is perpendicular to both $\vec{z}$ and $\vec{n}$ while the magnitude of P_s is in first approximation proportional to θ. A second consequence of the molecular chirality is the appearance of a helical superstructure in the Sm-C^* phase: the azimuthal tilt direction changes by a small amount when going from layer to layer. The corresponding helical pitch is usually of the order of a few μm or several hundred smectic layer thicknesses. Many compounds show at higher temperatures the smectic-A (Sm-A) phase in which $\vec{n}$ and $\vec{z}$ are parallel; accordingly, θ and P_s are zero and a helical structure does not exist.

The prediction and experimental confirmation of ferroelectric properties in the Sm-C^* phase of chiral molecules [1] has led to a large research effort concerning the Sm-C^* phase from both fundamental and applied viewpoints. An important discovery was the observation of several modifications of the Sm-C^* phase showing antiferroelectric (Sm-C^*_A,Sm-C^*_{AF}), ferrielectric (Sm-C^*_γ,Sm-C^*_{FI1}, Sm-C^*_{FI2}), or apparently both (Sm-C^*_α) properties [2,3].

Whereas in the conventional Sm-C^* phase the tilt direction, and thus the polarization direction, is locally constant, it is generally assumed that the antiferroelectric and ferrielectric properties of the new phases result from complex interlayer arrangements of the molecular tilt direction. The detailed structures are still unknown, with the exception of the antiferroelectric Sm-C^*_A phase, for which several experimental studies [2,4–6] indicated a layer-by-layer alternation of tilt and polarization direction by $\pm180°$. Recently, resonant x-ray scattering measurements [7,8] have provided direct structural evidence of periodicities corresponding to two-layer (Sm-C^*_A), three-layer (Sm-C^*_{FI1}), and four-layer (Sm-C^*_{FI2}) superlattices; for the (Sm-C^*_α) phase an incommensurate periodicity, varying between five and eight layers, was observed.

The Sm-C^*_α phase appears usually between the Sm-A and the conventional Sm-C^* phase, or, in some cases, between Sm-A and Sm-C^*_A or Sm-C^*_{FI}. Although it appears optically uniaxial in a polarizing microscope, Sm-C^*_α is a tilted phase, the tilt angle magnitude θ increases smoothly with decreasing temperature [9,10], similar to the case of a usual second-order Sm-A–Sm-C transition. On the other hand, the electro-optical and structural properties of this phase seem to change as a function of temperature and applied electric field [11,12], one can observe apparently antiferroelectric and ferrielectric behavior.

The first structural model proposed for the Sm-C^*_α phase is based on a one-dimensional Ising model exhibiting a Devil's staircase [13]; if the spin-up and the spin-down states of the Ising model are assigned to ''ferroelectric'' (same tilt direction in neighboring layers) and ''antiferroelectric'' (opposite tilt direction in neighboring layers) layer boundaries, an infinitely large number of structural states, characterized by different ratios of ferroelectric/antiferroelectric boundaries, is expected to occur in the Sm-C^*_α phase range [9,11]; as a driving force a competition between interactions favoring parallel or opposite tilt direction is assumed. A different proposed structure for the Sm-C^*_α phase results from a discrete phenomenological description [14], which takes into account competing nearest-neighbor and next-nearest-neighbor layer interactions, and from similar phenomenological models [15–17]. According to [14], the Sm-C^*_α phase is characterized by a helical structure with a very short and temperature dependent pitch which may be as small as

*Author to whom correspondence should be addressed. Electronic address: bahr@mailer.uni-marburg.de

 © 1999 The American Physical Society

only a few smectic layer thicknesses. Experimentally, sophisticated microscopic observations of thin droplets indicate a helical structure in the sub-μm range [18,19]. Also the resonant x-ray scattering measurements [7,8] provide strong support for the short-pitch helical structure. A third proposed structure for the Sm-C^*_α phase, resulting from circular dichroism measurements, consists of a dynamic helical structure with a very long average pitch [20]; this structure is partially supported by light scattering measurements [21].

We report here results of an ellipsometric study of freely suspended films of a chiral compound showing the phase sequence Sm-A – Sm-C^*_α – Sm-C^*. Freely suspended smectic films [22] consist of an integral number, variable between several hundred and only two, of smectic layers that are aligned parallel to the two free surfaces. By ellipsometric measurements on films consisting of only two, three, or four layers, the layer-by-layer alternation of the tilt direction in the Sm-C^*_A phase could be confirmed [6]. Concerning the other types of Sm-C^* phases we observed for several different compounds that ellipsometry on freely suspended films usually gave noisy and nonreproducible measurement values, possibly because of multi-domain structures and defects in the film; this behavior is very pronounced for the ferrielectric Sm-C^*_γ or Sm-C^*_{FI} phases. For the Sm-C^*_α phase, for one compound reproducible results could be obtained, the interpretation of which, however, was not unambiguous: while the discontinuous structural changes observed in thin films seemed to support the Devil's staircase structural model [23], the measurements on thick films could be interpreted as resulting from a short-pitch structure [24]. In the present study we report results obtained on a different compound which enabled high-resolution and well reproducible ellipsometric measurements in its Sm-C^*_α phase. A very characteristic temperature dependence of the ellipsometric quantities Δ and Ψ is observed which unequivocally proves the presence of a short-pitch helical structure.

II. EXPERIMENT

The compound under investigation, called ''11HFBBM7'' (the molecular structure is shown in Fig. 1), belongs to a group of four homologous series showing a variety of different Sm-C^* phases [25]; 11HFBBM7 possesses a several degrees broad Sm-C^*_α range, the transition temperatures of our sample are

$$\text{Cryst.} \underset{76°\text{C}}{\leftrightarrow} \text{Sm-}C^* \underset{94.5°\text{C}}{\leftrightarrow} \text{Sm-}C^*_\alpha \underset{98°\text{C}}{\leftrightarrow} \text{Sm-}A \underset{122°\text{C}}{\leftrightarrow} \text{Iso.}$$

Freely suspended films are drawn in the Sm-A phase using a rectangular, variable-area frame described in [26]. The typical film area is 5×10 mm. The beam of a HeNe-Laser passes through the film with an angle of incidence of 45°. Using a null-ellipsometer (details can be found in [27]) we determine the quantities Δ and Ψ which describe the state of polarization of the transmitted light. As usual, Δ corresponds to the phase difference between the p- and s-polarized components of the transmitted light, $\Delta=\delta_p-\delta_s$, and Ψ is related to the amplitudes $|T_{p,s}|$ of the p- and s-components, $\tan\Psi=|T_p|/|T_s|$. The polarization of the incident light is described by $\Delta=0$ and $\Psi=45°$.

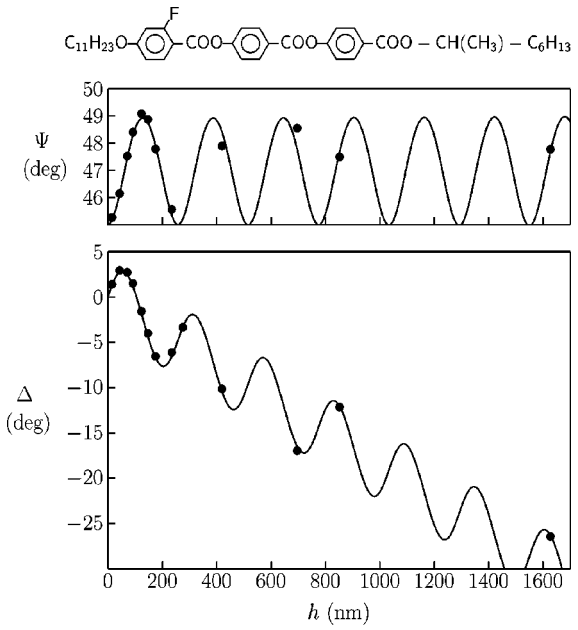

FIG. 1. Calculated curves [solid lines, see Eq. (1) and text] of the ellipsometric quantities Δ and Ψ as function of film thickness h. The ● symbols are values of Δ and Ψ that are measured near the high-temperature limit of the Sm-A phase (since the surface layers of 11HFBBM7 films are tilted even in this temperature range, the Δ values shown above correspond actually to the arithmetic mean of the measured Δ_+ and Δ_- values). The refractive index values n_e and n_o are varied until all experimentally measured Δ-Ψ pairs, for which the corresponding film thicknesses are initially not (or only approximately) known, can be placed onto the calculated curves.

A weak dc electric field (8 V/cm) is applied in the film plane and perpendicular to the plane of incidence (the plane containing the film normal and the incident laser beam). Values of Δ and Ψ are continuously collected while the temperature is changed at a slow constant rate (typically between 0.4 and 0.2 K/h). At least two, in most cases four measurement runs are conducted: we start with a cooling run which is followed by a heating run, then the polarity of the dc field is reversed and again a cooling and a heating run are recorded. The weak dc field is just sufficient to align the electric net polarization of the film, it is too weak to distort the internal film structure. In a nonhelicoidal Sm-C^* film, or in a film with $h\ll p$ (h being the film thickness and p the helical pitch), $\vec{n}$ would always lie within the plane of incidence and only two tilt directions (away from or towards the incident beam, depending on the polarity of the applied field) would be possible. We denote the values of Δ and Ψ belonging to the corresponding field polarities by subscripts ''+'' or ''−.''

An important point is the determination of the thickness of a given film. In very thin films (below ten layers), the quantization of the film thickness leads to a quantization of the measured Δ and Ψ values which can be directly related to the number of smectic layers of the film. Some hint about the film thickness is also obtainable from the intensity and color of the light which is reflected by the film when illuminated with white light [28]. However, the results of this study concern thicker films consisting of up to several hundred layers. The thickness of such films can be determined,

with an accuracy better than 5%, from the Δ and Ψ values measured at the high-temperature limit of the Sm-A phase, where the films correspond essentially to a thin uniaxial dielectric slab with its optical axis being parallel to the film normal. The complex transmission amplitude ratio of the p- and s-polarized components, T_p/T_s, of such a uniaxial slab, possessing two identical slab-ambient boundaries, is given by

$$\frac{T_p}{T_s}=\frac{(1-r_{01p}^2)e^{-i\beta_p}}{1-r_{01p}^2e^{-2i\beta_p}}\,\frac{1-r_{01s}^2e^{-2i\beta_s}}{(1-r_{01s}^2)e^{-i\beta_s}}. \tag{1}$$

Here, $r_{01p,s}$ are the Fresnel reflection coefficients for the air (medium 0)/film(medium 1) interface and $\beta_{p,s}$ are the phase shifts caused by the film; equations for $r_{01p,s}$ and $\beta_{p,s}$ are given in [27]. The values of Δ and $\tan\overline{\Psi}$ are then obtained from Eq. (1) as the argument (angle in complex plane) and the absolute value of T_p/T_s, i.e., $\Delta=\arg(T_p/T_s)$ and $\overline{\Psi}=\arctan(|T_p/t_s|)$. For fixed angle of incidence and light wavelength, the shape of the Δ versus h and Ψ versus h curves (h being the film thickness) depends only on the refractive indices n_e (or $n_\parallel$) and n_o (or $n_\perp$) of the liquid crystal. If these values are not known, a number of 15 to 20 Δ-Ψ pairs, measured on films of different thicknesses, is usually sufficient to fit, by varying n_e and n_o, the calculated curves to the measured Δ and Ψ values. At the beginning of this procedure, the film thicknesses belonging to the measured Δ-Ψ pairs are of course not known; of special importance are therefore the Δ-Ψ pairs obtained from thin films, where one can get with some experience an approximate film thickness by inspecting the film by the eye (from color and intensity of the reflected light). The result obtained for 11HFBBM7 is shown in Fig. 1; the refractive index values that gave the best fit are $n_e=1.545$ and $n_o=1.415$. The assignment of a film thickness to a given film based on the calculated curves shown in Fig. 1 has to be checked about its consistency, in the present study this check is provided by a detailed comparison of the measured $\Delta(T)$ and $\Psi(T)$ values of different films with values calculated for model films as described in Sec. IV.

If the thickness of a single smectic layer is known (we estimate 4 nm from the molecular length of 11HFBBM7), the nm or Å units of the film thickness scale can be transformed into layer-number units. Because the most significant results of the present study are obtained for films with thicknesses between 40 and 400 layers, the knowledge of the exact number of layers of a given film is not crucial.

III. RESULTS OF ELLIPSOMETRIC MEASUREMENTS

Figure 2 shows the temperature dependence of $\Delta_{+,-}$ and $\Psi_{+,-}$ for a 850 nm ($\approx$213 layers) thick film. Above 98°C, in the temperature range of the bulk Sm-A phase, we observe $\Psi_+=\Psi_-$ and an almost constant difference between Δ_+ and Δ_-, which results from tilted surface layers on a ''bulk'' Sm-A film. The occurrence of such a surface-induced tilt is a quite common phenomenon in compounds possessing a bulk Sm-C phase [29–31]. In 11HFBBM7, the difference between Δ_+ and Δ_- persists up to the bulk Sm-A–isotropic transition temperature, where the film ruptures, i.e., the surface layers are tilted in the whole temperature range of the bulk Sm-A phase.

Below 98 °C the behavior of Δ and Ψ changes, as is shown in detail in Fig. 3: The two Δ curves show a characteristic oscillation with peaks where the two curves touch or come close to each other. At the same temperatures, where the Δ curves show their peaks, the two Ψ curves cross each other and show an additional crossing just between two Δ peaks. The distance on the temperature scale between these features becomes smaller with decreasing temperature. The behavior changes again at 94.5 °C where suddenly large differences $|\Delta_+-\Delta_-|$ and $|\Psi_+-\Psi_-|$ appear, which are followed by two oscillations or crossings, until at lower temperatures only slight variations of $\Delta_{+,-}$ and $\Psi_{+,-}$ remain.

Figures 4 and 5 show how these features change when the film thickness is varied. It seems that the number of Δ-oscillations or Ψ-crossings is approximately proportional to the thickness of the films.

We will describe in Sec. IV how all observations can be explained by a structural model that consists essentially of a short-pitch helical precession of the tilt direction around the layer normal. Already without a detailed comparison of measured Δ and Ψ values and values calculated from model films, we can exclude for 11HFBBM7 two of the structural models proposed for the Sm-C_α^* phase described in Sec. I.

In the Devil's staircase structure derived from the one-dimensional Ising model, only two tilt directions, opposite to each other, are possible, i.e., locally the molecules in different layers tilt within a common plane (there may be a helicoidal twist of the tilt plane but only over distances of the order of micrometers). Any nonzero net polarization would point in a direction perpendicular to the tilt plane and because of the applied dc field the tilt plane would coincide with the plane of incidence (the plane containing the film normal and the incident laser beam). For such a film structure we would obtain always $\Psi_+=\Psi_-$ (as is indeed observed in the Sm-A range, although the surface layers are tilted) independently from the actual tilt direction in each layer (which would be either towards or away from the incident beam). Since we observe clearly $\Psi_+\neq\Psi_-$, the tilt direction must in some layers deviate from the plane of incidence, and this is (in films as thin as 40 to 60 layers) not compatible with the Devil's staircase model.

Concerning the dynamic long-pitch helical structure, a helix possessing a pitch of some μm would hardly be seen in a 100 or 200 nm thick film and the film should yield then similar results as a usual Sm-C^* phase. Dynamic changes of the helical structure could result in noisy or unreproducible measurements. Both expectations are in contrast to our measurements, which are well reproducible in successive heating and cooling runs and deviate clearly from measurements obtained on usual Sm-C^* phases (see, e.g., [30,31]).

IV. COMPARISON WITH RESULTS FROM MODEL FILMS

Can a helical precession of the tilt direction with a small and temperature-dependent pitch produce values of Δ and Ψ as measured in the Sm-C_α^* phase of 11HFBBM7? To answer this question we have to compare our measured values with Δ and Ψ values calculated for model films possessing appropriate structures. In the following, we assume that each smectic layer of a model film corresponds to a thin uniaxial dielectric slab possessing refractive indices $n_e=1.545$ and

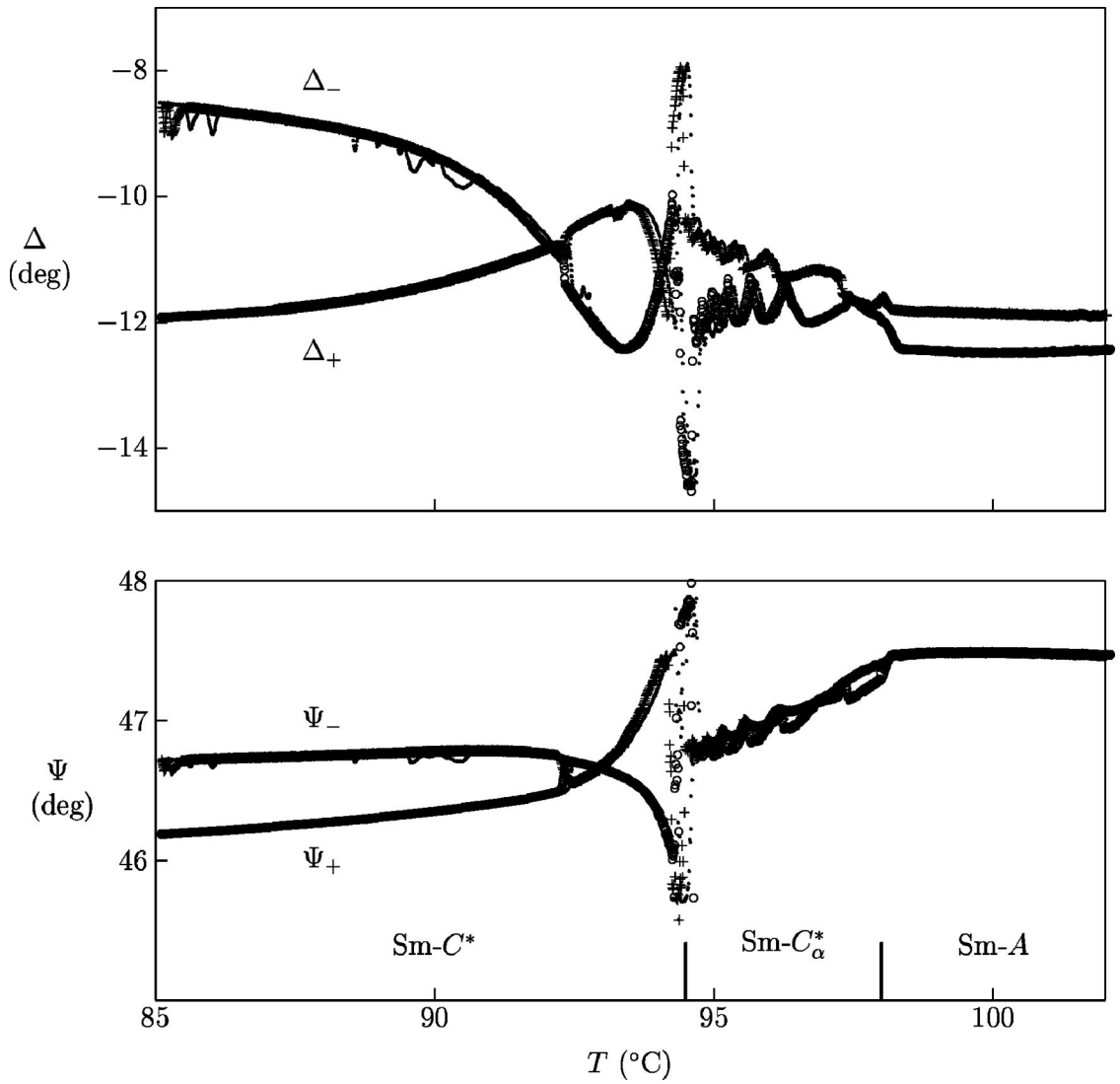

FIG. 2. Temperature dependence of the ellipsometric quantities $\Delta_{+,-}$ and $\Psi_{+,-}$ in the Sm-C^*, Sm-C^*_α, and Sm-A phases of a 213-layer film of 11HFBBM7. Each diagram shows two cooling runs ($\bigcirc$: $\Delta_+, \Psi_+, +$: Δ_-, Ψ_-) and two heating runs (small dots, mostly not distinguishable from the cooling runs).

$n_o = 1.415$. The orientation of the optical axis of each layer is determined by angles θ_i and ϕ_i which give the tilt angle magnitude and the azimuthal tilt direction in the ith layer. The net polarization $\vec{P}_{s,net}$ of the complete film is calculated and the whole structure is rotated until $\vec{P}_{s,net}$ would be parallel to an external dc field which is assumed to be applied perpendicular to the plane of incidence. The values $\Delta_{+,-}$ and $\Psi_{+,-}$ are then calculated where the subscripts $+,-$ refer to two opposite orientations of $\vec{P}_{s,net}$ corresponding to the two polarities of the virtually applied field. Details of the calculation process, which employs the 4×4-matrix method [32], are given in [33].

We first consider the effect of a helicoidal precession of the tilt direction along the layer normal using a simple model film consisting of 100 layers possessing a thickness $d = 4$ nm. The tilt angle between the optical axis and the layer normal is set (arbitrarily) to 16° in each layer. The values of $\Delta_{+,-}$ and $\Psi_{+,-}$ are then calculated as function of the angle α, which corresponds to the difference between the tilt directions of neighboring layers. Figure 6 shows the result in the range from $\alpha = 0$ (same tilt direction in all layers, infinitely large pitch) to $\alpha = 45°$ (helical pitch corresponding to eight layers). It is obvious that the variation of the azimuthal difference α (or, equivalently, of the helical pitch p) in the simple model film leads, on a qualitative level, to quite similar Δ-oscillations or Ψ-crossings as observed experimentally. Even from some subtle features of the calculated curves one can find traces in the measurements: as is shown in Fig. 6, the contact of the two oscillating Δ curves consists actually of a double crossing, i.e., a simple intersection and a discontinuous jump of the two curves; experimentally, this behavior is seen in Fig. 4 (for the 44-layer film) and, to some extent, in Fig. 3.

As can be seen in Fig. 6, the Δ- and Ψ-oscillations are placed equidistantly on the α-scale. The behavior of $\Delta(\alpha)$ and $\Psi(\alpha)$ is a result of a compatibility effect involving two length scales: the helical pitch p and the film thickness h. The difference between Δ_+ and Δ_- becomes small whenever

$$h = np \quad \text{with } n = 1,2,3,\ldots, \tag{2}$$

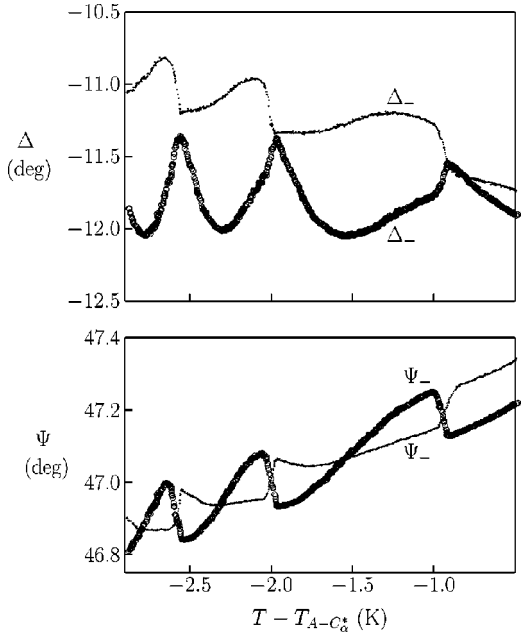

FIG. 3. Oscillation and crossing behavior of $\Delta_{+,-}$ and $\Psi_{+,-}$ within the Sm-C^*_α phase of a 213-layer film of 11HFBBM7. $T_{A-C^*_\alpha}$ is the Sm-A–Sm-C^*_α transition temperature.

i.e., when the film thickness is an integral multiple of the helical pitch, and $|\Delta_+ - \Delta_-|$ reaches a maximum in between. If we measure p and h in layer-number units, we obtain $h = np$ whenever $\alpha = n(2\pi/h)$. For our 100-layer model film this condition results in $\alpha/n = 3.6°$, which is exactly the distance between the oscillations of the calculated Δ and Ψ curves shown in Fig. 6.

The shape of the Δ and Ψ curves is additionally influenced by reorientation effects caused by the applied field. Whenever α moves through $n \times 3.6°$, the net polarization of the film is inverted and in the presence of an applied dc field the whole structure changes its azimuthal orientation by 180°. These reorientations can be seen in the calculated curves as discontinuous jumps (pronounced for Ψ, small for Δ), which are smeared out, but to some extent still discernible, in the experimental curves (see Fig. 3).

As described above, the introduction of a short helical pitch in a simple 100-layer model film explains many of the experimentally observed features. Our ellipsometric measurements thus strongly support the short-pitch structural model for the Sm-C^*_α phase of 11HFBBM7. The next step consists in an attempt of a quantitative fit of the experimental curves with the aim to obtain the temperature dependence of the helical pitch in the Sm-C^*_α phase. Besides a temperature dependence of α (or p) we have to consider a temperature dependence of the tilt angle magnitude θ and possible surface effects resulting in a temperature-dependent structural profile across the film.

The temperature dependence of θ can be obtained from the Ψ versus T curves of thick films in conjunction with the amplitude of the oscillations of the Δ versus T curves. As is seen for the 407-layer film data of Fig. 5, there is an overall decrease of Ψ with decreasing temperature, which starts at the Sm-A to Sm-C^*_α transition. This overall Ψ-decrease reflects the decrease of the film thickness caused by the molecular tilt angle θ: in a simple hard-rod approximation, the thickness d of a single smectic layer would decrease with $\cos\theta$, i.e.,

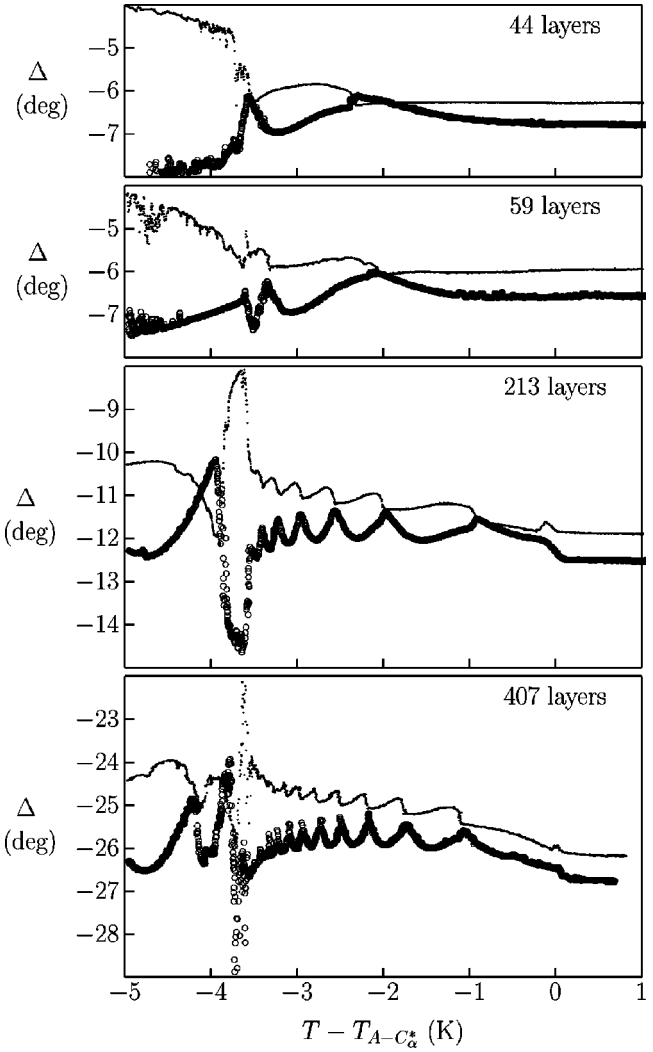

FIG. 4. Temperature dependence of the ellipsometric quantities Δ_+ (○) and Δ_- (·) in the Sm-C^*_α phase of various films of 11HFBBM7. The film thicknesses (±5%) are (from above): 177 nm, 237 nm, 850 nm, 1.63 μm, the corresponding approximate number of layers (obtained with a single layer thickness of 4 nm) is given in each diagram; $T_{A-C^*_\alpha}$ is the Sm-A–Sm-C^*_α transition temperature, the transition to the usual Sm-C^* phase occurs at $T - T_{A-C^*_\alpha} \approx -3.5$ K.

$$\theta = \arccos\left(\frac{d}{d_0}\right), \tag{3}$$

with d_0 being the layer thickness for $\theta = 0$. Experimentally, x-ray studies have been reported in which d and θ were measured independently and which either directly confirmed Eq. (3) [34] or led to a slightly modified relation [35]:

$$\theta = R \arccos\left(\frac{d}{d_0}\right), \tag{4}$$

with $R \approx 1.2$. Figure 7 gives the decrease of the thickness of 407-layer film determined from the data shown in Fig. 5 and

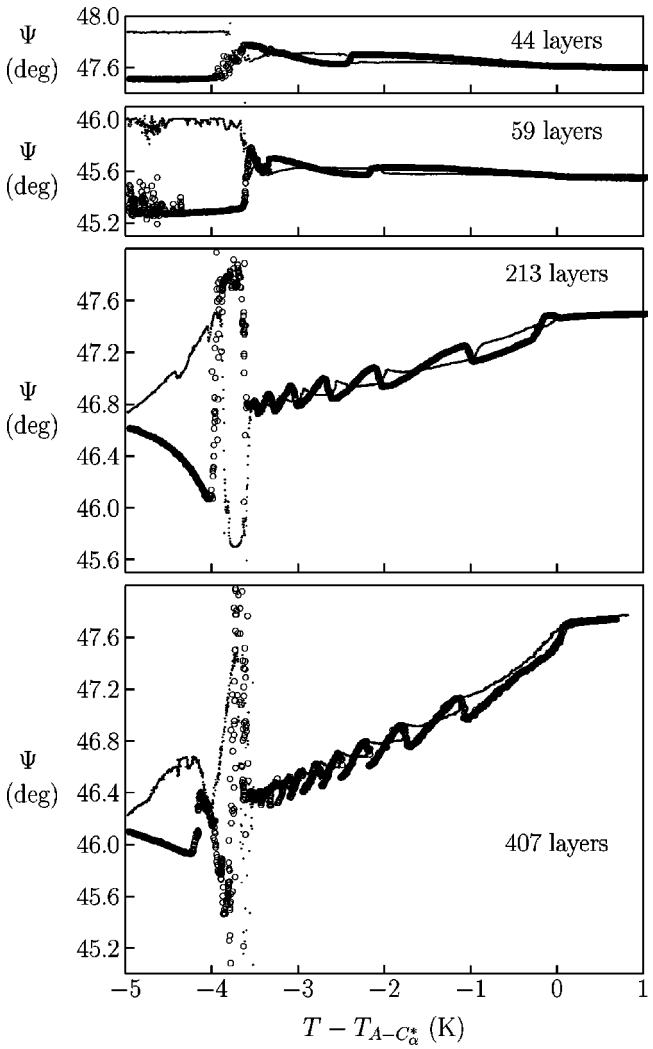

FIG. 5. Temperature dependence of the ellipsometric quantities Ψ_+ (○) and Ψ_- (·) in the Sm-C^*_α phase of various films of 11HFBBM7 (see caption of Fig. 4).

the resulting values of θ according to Eq. (3). It is well known that the tilt angle determined as described above from the smectic layer shrinkage is usually smaller than the tilt angle of the optical axis measured by optical methods, indicating that the aromatic cores are more tilted than the flexible alkyl chains [36,37]. Indeed we find that the θ values resulting from Eq. (3) are too small to reproduce the ''amplitude'' of the Δ oscillations shown in Fig. 4. A reasonable fit is possible if we determine θ from Eq. (4) with $R \geqslant 1.4$.

In the following we assume that the temperature dependence of θ in all films is described by the θ versus T curve obtained from the thickness decrease of the 407-layer film according to Eq. (4) with $R=1.4$ (see Fig. 7). We further assume that θ shows the same value in all layers of a given film, with the only exception of the two surface layers, for which we set θ to a constant value of 30° corresponding approximately to the difference $|\Delta_+ - \Delta_-|$ measured for all films in the bulk Sm-A temperature range.

Next we have to determine the temperature dependence of the angle α that corresponds to the azimuthal difference of the tilt direction in neighboring layers. The number of oscillations in the measured Δ curves determines the width $\Delta\alpha$

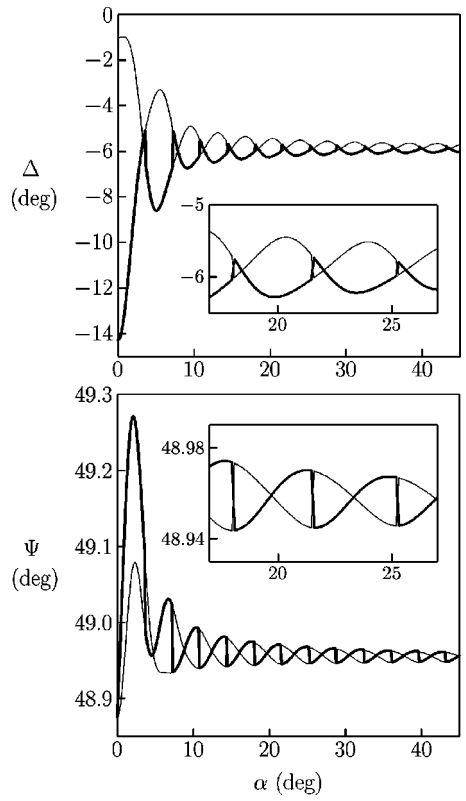

FIG. 6. Calculated ellipsometric quantities Δ_+, Ψ_+ (thick lines) and Δ_-, Ψ_- (thin lines) as a function of angle α which corresponds to the difference of the azimuthal tilt directions in neighboring layers. The values are calculated for a 100-layer model film as described in the text. The insets give an enlarged view of the Δ and Ψ oscillations.

on the α-scale over which α varies in the Sm-C^*_α phase; e.g., we observe seven oscillations for the 213-layer film resulting in $\Delta\alpha = (360°/213)7 = 11.8°$, a similar value is obtained for all film thicknesses. The main difficulty is to determine the absolute values of α at the high- and low-temperature limits, α_{ht} and $\alpha_{lt} = \alpha_{ht} - \Delta\alpha$. This difficulty arises especially for large α values and thick films, e.g., in a

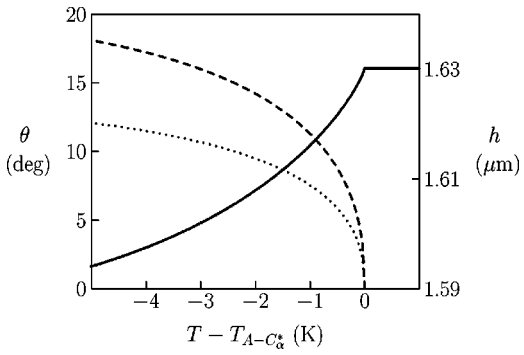

FIG. 7. Temperature dependence of the thickness h (solid line) of the 407-layer film determined from the Ψ data shown in Fig. 5; the dotted line gives the corresponding values of the tilt angle θ according to the hard-rod approximation [Eq. (2)]. The dashed line gives the θ values resulting from Eq. (3) with $R=1.4$, this θ vs T curve is taken as a basis for the Δ and Ψ calculations shown in Figs. 8 and 9.

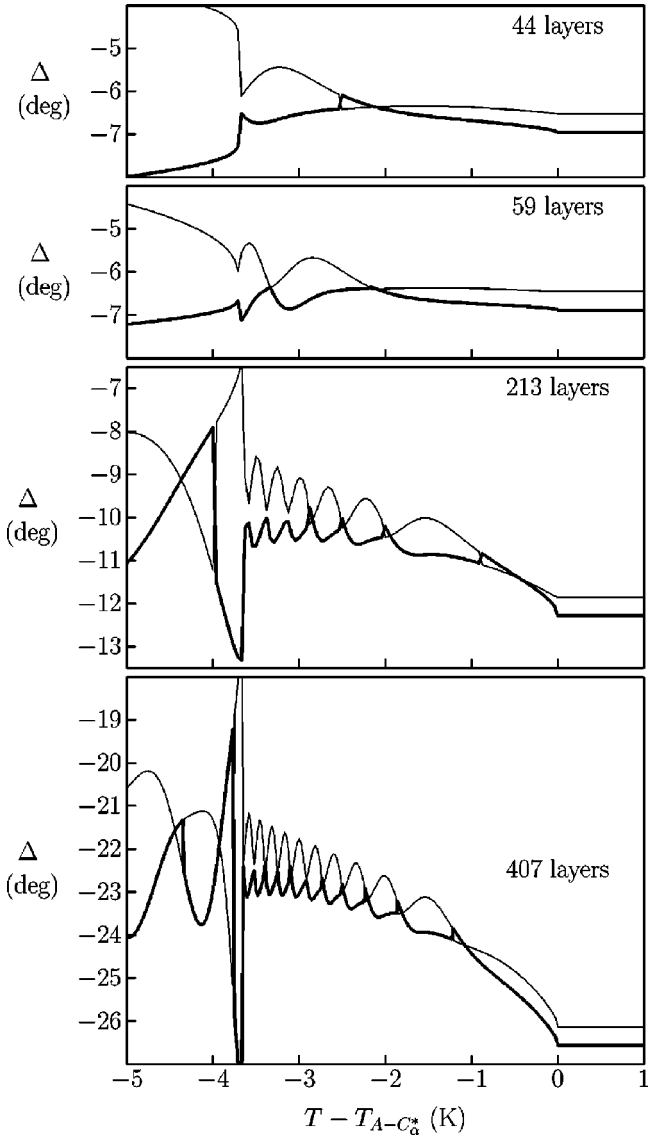

FIG. 8. Calculated ellipsometric quantities Δ_+ (thick lines) and Δ_- (thin lines) as a function of temperature for four model films (see text) corresponding to the experimentally studied films shown in Fig. 4; the temperature variation is obtained using a temperature variation of the angle α which is shown in Fig. 10.

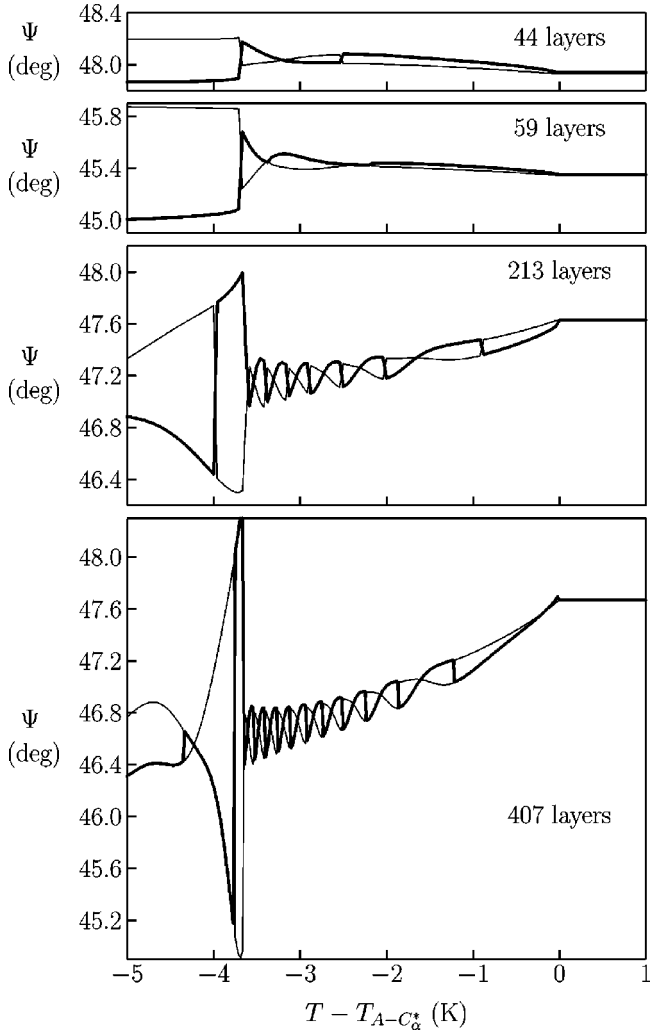

FIG. 9. Calculated ellipsometric quantities Ψ_+ (thick lines) and Ψ_- (thin lines) as a function of temperature for four model films (see text) corresponding to the experimentally studied films shown in Fig. 5; the temperature variation is obtained using a temperature variation of the angle α which is shown in Fig. 10.

100-layer film it is hardly possible to distinguish the Δ oscillations in the range from, say, $\alpha = 35°$ to 40° from the oscillations in the range from $\alpha = 40°$ to 45° (see Fig. 6). However, our measured data for the 44- and 60-layer films are satisfactorily reproduced by the calculated values only if we let α vary with temperature in the range from $\alpha_{ht} \approx 18°$ to $\alpha_{lt} \approx 7°$. Nearly the same $\alpha(T)$ dependencies reproduce our data well for the 213- and 407-layer films, but for these films the $\alpha(T)$ curves could be shifted, in steps of (360/213) respectively (360/407) degrees, to somewhat larger α values without significantly changing the calculated Δ and Ψ curves. The measured data in the range of the Sm-C^* phase are reproduced with a slight temperature variation of α from 6° to 4°.

Figures 8 and 9 show the Δ and Ψ curves which were calculated as described above; Fig. 10 gives the corresponding temperature dependence of α which was used for the calculation. Although the qualitative resemblance to the measured values (see Figs. 4 and 5) is striking, a complete quantitative correspondence is not achieved, which may be due to several reasons: First, the division of a N-layer film into two surface layers possessing a constant tilt magnitude θ, and $N-2$ interior layers, in which θ is dependent on temperature but not on the position of the layer inside the film, is certainly an oversimplification. When the Sm-C_α^* to Sm-C^* transition is approached from above, probably a Sm-C^*-like surface phase, characterized by a smaller α and larger θ value compared to the interior Sm-C_α^* phase, grows into the film interior resulting in a θ and α profile across the film; this behavior can be seen in the Δ data of the 407-layer film (Fig. 4) where the two Δ curves clearly separate from each other as the transition to the Sm-C^* phase is approached [38]. Second, the calculation of the Δ and Ψ values shown in Figs. 8 and 9 was done treating each smectic layer as a uniaxial slab whereas in fact a Sm-C layer is optically biaxial [39]. Third, the principal index values n_o and n_e were assumed as temperature independent. Thus, a further refine-

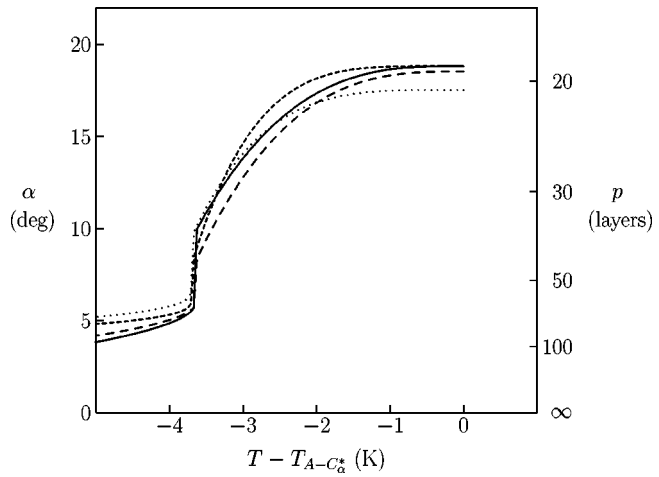

FIG. 10. Temperature dependence of the angle α (corresponding to the difference between the azimuthal tilt directions in neighboring layers), which was used to calculate the Δ and Ψ curves shown in Figs. 8 and 9 (dots: 44-layer film, short dashes: 59-layer film, long dashes: 213-layer film, solid line: 407-layer film). The right-hand scale gives the corresponding helical pitch p in units of smectic layers.

ment of our model films would probably result in a still better agreement of measured and calculated Δ and Ψ values but the considerably larger calculation and fitting effort would yield only minor additional physical information.

The essential result of our study is that the measured ellipsometric values of the Sm-C^*_α phase are well explained by a temperature dependent short-pitch helical structure. Although ellipsometry suffers generally from an inversion problem, i.e., different refractive index profiles may lead to similar Δ and Ψ values, it is hardly possible to consider a reasonable alternative structure of the Sm-C^*_α phase which can result in the observed behavior of Δ and Ψ. The existing alternative Sm-C^*_α models, the dynamical long-pitch structure and the Devil's staircase based on the one-dimensional Ising model, are definitely not in accordance with our measurements.

The temperature dependence of the helical pitch p that gives the best reproduction of our measured values is shown in Fig. 10. There are slight differences between films of different thickness but all measurements, comprising a thickness range of roughly 40 to 400 layers, are reproduced by an essentially similar temperature dependence of the helical pitch: p increases nonlinearly with decreasing temperature from $\approx$20 layer thicknesses ($\approx$80 nm) just below the transition from the Sm-A phase to $\approx$40 layers ($\approx$160 nm) near the transition to Sm-C^* phase. The Sm-C^*_α–Sm-C^* transition is characterized by a steep, maybe discontinuous increase of p to $\approx$300 nm; within the Sm-C^* phase range p increases further to $\approx$400 nm.

The short-pitch helical structure of the Sm-C^*_α phase has now been confirmed by three different experimental methods: direct optical observation of Friedel fringes at the free surface of very flat drops [18,19], polarization-analyzed resonant x-ray scattering [7,8] in freely suspended films, and ellipsometry of freely suspended films. The temperature dependence of the helical pitch p observed in the present study is at variance with the results of the x-ray study: for the

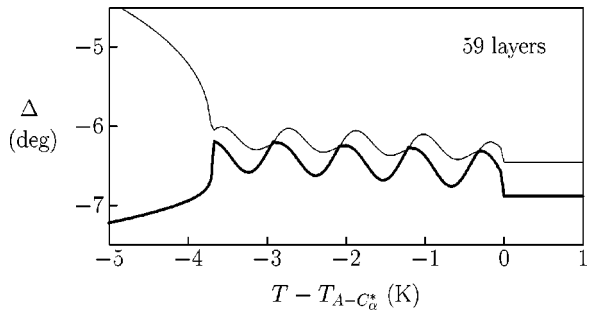

FIG. 11. Calculated ellipsometric quantities Δ_+ (thick line) and Δ_- (thin line) as a function of temperature for a 59-layer model film, in which the helical pitch in the Sm-C^*_α decreases linearly from eight to five layer thicknesses with decreasing temperature as was observed for the compound 10OTBBB1M7 by resonant x-ray scattering. All other parameters of the model film (i.e., the pitch in the Sm-C^* phase and temperature dependence of the tilt angle) are left unchanged.

compound studied in [7,8], 10OTBBB1M7 [40], p is reported to decrease linearly, from eight to five layers, with decreasing temperature. For comparison we have calculated the temperature dependence of Δ and Ψ for such a linear decrease of p in the Sm-C^*_α range for a 59-layer model film (in which all other properties are left as described above). The result is shown in Fig. 11. It is obvious that the calculated Δ and Ψ values do not describe the behavior which is experimentally observed (see 59-layer data in Fig. 4) for the compound under investigation, 11HFBBM7.

As in the case of 11HFBBM7, the Sm-C^*_α phase in 10OTBBB1M7 occurs between the Sm-A and the Sm-C^* phase. Intuitively, one would expect p to increase when the transition to the Sm-C^* phase, where p usually amounts to at least some hundred nm, is approached (and indeed this behavior is observed in the present study). The Sm-C^* phase width in 10OTBBB1M7 amounts, however, only to 1 K and then a transition to a Sm-C^*_{FI2} phase occurs, for which a 4-layer pitch is observed [7,8]. In 11HFBBM7, the Sm-C^* phase below the Sm-C^*_α phase is at least 17 K broad and it is not known if metastable Sm-C^*_{FI} or Sm-C^*_A phases exist at lower temperatures. The absence of these phases may be due to the same reasons which result in the opposite temperature dependence and the generally larger values of p in the Sm-C^*_α phase of 11HFBBM7 compared to 10OTBBB1M7.

In the studies [18,19] based on the direct optical observation of Friedel fringes at the free surface, also 10OTBBB1M7 and homologous compounds are investigated. If p is smaller than ten layer thicknesses, the relation between p and the observed optical period is not simple [19] but the results of these direct optical observations are in accordance with the x-ray results. In [18,19] a pronounced dependence of the observed optical period on the thermal history of the sample was found. It seems, however, that this dependence is not an intrinsic property of the Sm-C^*_α phase but rather a result of the experimental conditions in [18,19]: in both the present study and the x-ray measurements, where freely suspended films are used, a dependence on the thermal history is not observed and heating and cooling runs yield well reproducible results.

V. CONCLUSION

We have reported an ellipsometric study of freely suspended films of the compound 11HFBBM7 possessing the phase sequence Sm-A –Sm-C^*_α – Sm-C^*. A detailed comparison of the measured ellipsometric quantities with values resulting from model films provides strong support of the short-pitch helical structure of the Sm-C^*_α phase and rules out the the dynamical long-pitch and the Ising Devil's staircase structural models. The best reproduction of the experimental data of films in the thickness range from 40 to 400 layers is obtained with a temperature dependent helical pitch which increases in the Sm-C^*_α phase from $\approx$20 to $\approx$40 smectic layer thicknesses with decreasing temperature. This behavior differs from the temperature dependence of the pitch in the Sm-C^*_α phase of the compound 10OTBBB1M7 for which x-ray measurements indicate a decrease from eight to five layer thicknesses with decreasing temperature. The different temperature dependence and magnitude of the pitch in the two compounds may be related to their phase sequences, i.e., the absence or occurrence of low-temperature ferrielectric and antiferroelectric phases and the width of the ferroelectric Sm-C^* phase. More experimental studies of different compounds are needed.

According to the phenomenological model [14] the short-pitch helical structure of the Sm-C^*_α phases arises from the frustration of competing nearest-neighbor and next-nearest-neighbor layer interactions favoring parallel or opposite tilt directions. The molecular chirality adds just a minor modulation and determines the sense of the resulting helical structure; thus, the helical pitch in the Sm-C^*_α should essentially not depend on the enantiomeric excess. Future experimental studies could address this point by measurements on chiral-racemic mixtures with varying enantiomeric excess.

ACKNOWLEDGMENTS

This work was supported by the Deutsche Forschungsgemeinschaft (Grant No. Ba1048/5) and the Fonds der Chemischen Industrie. Ch. B. is grateful to the Deutsche Forschungsgemeinschaft for financial support. Special thanks are due to M. Čepič for helpful discussions on optical measurements and the structure of the Sm-C^*_α phase.

[1] R.B. Meyer, L. Liebert, L. Strzelecki, and P. Keller, J. Phys. (France) Lett. **36**, L69 (1975).
[2] A.D.L. Chandani, E. Gorecka, Y. Ouchi, H. Takezoe, and A. Fukuda, Jpn. J. Appl. Phys. **28**, L1265 (1989).
[3] A. Fukuda, Y. Takanishi, T. Isozaki, K. Ishikawa, and H. Takezoe, J. Mater. Chem. **4**, 997 (1994).
[4] Y. Galerne and L. Liebert, Phys. Rev. Lett. **66**, 2891 (1991).
[5] Y. Takanishi, H. Takezoe, A. Fukuda, and J. Watanabe, Phys. Rev. B **45**, 7684 (1992).
[6] Ch. Bahr and D. Fliegner, Phys. Rev. Lett. **70**, 1842 (1993).
[7] P. Mach, R. Pindak, A.-M. Levelut, P. Barois, H.T. Nguyen, C.C. Huang, and L. Furenlid, Phys. Rev. Lett. **81**, 1015 (1998).
[8] P. Mach, R. Pindak, A.-M. Levelut, P. Barois, H. T. Nguyen, H. Baltes, M. Hird, K. Toyne, A. Seed, J. W. Goodby, C. C. Huang, and L. Furenlid, Phys. Rev. E **60**, 6793 (1999).
[9] T. Isozaki, K. Hiraoka, Y. Takanishi, H. Takezoe, A. Fukuda, Y. Suzuki, and I. Kawamura, Liq. Cryst. **12**, 59 (1992).
[10] M. Škarabot, M. Čepič, B. Žekš, R. Blinc, G. Heppke, A.V. Kityk, and I. Muševič, Phys. Rev. E **58**, 575 (1998).
[11] Y. Takanishi, K. Hiraoka, V.K. Agrawal, H. Takezoe, A. Fukuda, and M. Matsushita, Jpn. J. Appl. Phys. **30**, 2023 (1991).
[12] K. Hiraoka, Y. Takanishi, K. Skarp, H. Takezoe, and A. Fukuda, Jpn. J. Appl. Phys. **30**, L1819 (1991).
[13] P. Bak and R. Bruinsma, Phys. Rev. Lett. **49**, 249 (1982).
[14] M. Čepič and B. Žekš, Mol. Cryst. Liq. Cryst. Sci. Technol., Sect. A **263**, 61 (1995).
[15] V.L. Lorman, Mol. Cryst. Liq. Cryst. Sci. Technol., Sect. A **262**, 437 (1995).
[16] S.A. Pikin, S. Hiller, and W. Haase, Mol. Cryst. Liq. Cryst. Sci. Technol., Sect. A **262**, 425 (1995).
[17] A. Roy and N. Madhusudana, Europhys. Lett. **36**, 221 (1996).
[18] V. Laux, N. Isaert, H.T. Nguyen, P. Cluzeau, and C. Destrade, Ferroelectrics **179**, 25 (1996).
[19] V. Laux, N. Isaert, G. Joly, and H.T. Nguyen, Liq. Cryst. **26**, 361 (1999).
[20] K. Yamada, Y. Takanishi, K. Ishikawa, H. Takezoe, A. Fukuda, and M.A. Osipov, Phys. Rev. E **56**, R43 (1997).
[21] D. Konovalov and S. Sprunt, Phys. Rev. E **58**, 6869 (1998).
[22] C.Y. Young, R. Pindak, N.A. Clark, and R.B. Meyer, Phys. Rev. Lett. **40**, 773 (1978).
[23] Ch. Bahr, D. Fliegner, C.J. Booth, and J.W. Goodby, Phys. Rev. E **51**, R3823 (1995).
[24] B. Rovšek, M. Čepič, and B. Žekš, Phys. Rev. E **54**, R3113 (1996).
[25] V. Faye, J.C. Rouillon, C. Destrade, and H.T. Nguyen, Liq. Cryst. **19**, 47 (1995).
[26] P. Pieranski, L. Beliard, J.-Ph. Tournellec, X. Leoncini, C. Furtlehner, H. Dumoulin, E. Riou, B. Jouvin, J.-P. Fénerol, Ph. Palaric, J. Heuving, B. Cartier, and I. Kraus, Physica A **194**, 364 (1993).
[27] Ch. Bahr and D. Fliegner, Phys. Rev. A **46**, 7657 (1992).
[28] E.B. Sirota, P.S. Pershan, L.B. Sorensen, and J. Collett, Phys. Rev. A **36**, 2890 (1987).
[29] S. Heinekamp, R.A. Pelcovits, E. Fontes, E.Y. Chen, R. Pindak, and R.B. Meyer, Phys. Rev. Lett. **52**, 1017 (1984).
[30] S.M. Amador, and P.S. Pershan, Phys. Rev. A **41**, 4326 (1990).
[31] Ch. Bahr, C.J. Booth, D. Fliegner, and J.W. Goodby, Phys. Rev. Lett. **77**, 1083 (1996).
[32] D.W. Berreman, J. Opt. Soc. Am. **62**, 502 (1972).
[33] D. Schlauf, Ch. Bahr, V.K. Dolganov, and J.W. Goodby, Eur. Phys. J. B **9**, 461 (1999).
[34] B.M. Ocko, A.R. Kortan, R.J. Birgeneau, and J.W. Goodby, J. Phys. (Paris) **45**, 113 (1984).
[35] C.R. Safinya, M. Kaplan, J. Als-Nielsen, R.J. Birgeneau, D. Davidov, J.D. Litster, D.L. Johnson, and M.E. Neubert, Phys. Rev. B **21**, 4149 (1980).
[36] R. Bartolino, J. Doucet, and G. Durand, Ann. Phys. (N.Y.) **3**, 389 (1978).
[37] E.N. Keller, E. Nachaliel, D. Davidov, and C. Böffel, Phys. Rev. A **34**, 4363 (1986).

[38] In this context it is interesting to note that a pretransitional growth of the tilted surface domain is not observed when the Sm-A to Sm-C^*_α transition is approached from above, as can be seen in Figs. 2 and 4 where the difference between Δ_+ and Δ_- in the bulk Sm-A temperature remains essentially constant until the bulk transition to the Sm-C^*_α phase is reached. This may be an indication that the tilted surface phase that is present in the bulk Sm-A temperature range is of the usual Sm-C^* and not Sm-C^*_α type.

[39] The reason for this uniaxial approximation is a considerable simplification of the calculation: Δ and Ψ of an arbitrary system of uniaxial layers can be calculated by the 4×4 matrix method using analytical steps only [H. Wöhler, G. Haas, M. Fritsch, and D.A. Mlynski, J. Opt. Soc. Am. A **5**, 1554 (1988)], whereas biaxial layers require numerical procedures.

[40] 10OTBBB1M7 belongs to a series of thiobenzoate compounds described in H.T. Nguyen, J.C. Rouillon, P. Cluzeau, G. Sigaud, C. Destrade, and N. Isaert, Liq. Cryst. **17**, 571 (1994).